

# *Gaia*, an all-sky survey for standard photometry

J.M. Carrasco, M. Weiler, C. Jordi, and C. Fabricius

Institut de Ciències del Cosmos, Universitat de Barcelona (IEEC-UB), Martí Franquès 1, E-08028 Barcelona, Spain, carrasco@fqa.ub.edu

## Abstract

*Gaia* ESA's space mission (launched in 2013) includes two low resolution spectroscopic instruments (one in the blue, BP, and another in the red, RP, wavelength domains) to classify and derive the astrophysical parameters of the observed sources. As it is well known, *Gaia* is a full-sky unbiased survey down to about 20th magnitude. The scanning law yields a rather uniform coverage of the sky over the full extent (a minimum of 5 years) of the mission. *Gaia* data reduction is a global one over the full mission. Both sky coverage and data reduction strategy ensure an unprecedented all-sky homogeneous spectrophotometric survey. Certainly, that survey is of interest for current and future on-ground and space projects, like LSST, PLATO, EUCLID and J-PAS/J-PLUS among others. These projects will benefit from the large amount (more than one billion) and wide variety of objects observed by *Gaia* with good quality spectrophotometry. Synthetic photometry derived from *Gaia* spectrophotometry for any passband can be used to expand the set of standard sources for these new instruments to come. In the current *Gaia* data release scenario, BP/RP spectrophotometric data will be available in the third release (in 2018, TBC). Current preliminary results allow us to estimate the precision of synthetic photometry derived from the *Gaia* data. This already allows the preparation of the on-going and future surveys and space missions. We discuss here the exploitation of the *Gaia* spectrophotometry as standard reference due to its full-sky coverage and its expected photometric uncertainties derived from the low resolution *Gaia* spectra.

## 1 Introduction

*Gaia* will accurately observe more than one billion sources with accurate photometry<sup>1</sup> that will become standards for future ground and space-based instruments. Thus, there is a clear interest in the astronomical community to have realistic estimations of the *Gaia* spectrophotometric errors in order to evaluate the use of *Gaia* data for calibration and standardization

---

<sup>1</sup>For a complete description of the *Gaia* photometric instrument we refer to [2, 4, 5].

purposes. We discuss here the expected number of available sources and their quality at different sky positions. We also remind to relate *Gaia* with other photometric system, it could be very useful to use the photometric relationships derived during the first *Gaia* data release (see [2, 10] and the on-line documentation of the first *Gaia* release<sup>2</sup>).

## 2 Synthetic photometry from BP/RP

BP/RP photometric passbands and their spectra are planned to be published in the second and third *Gaia* release<sup>3</sup>, respectively. In order to provide now estimations of the signal-to-noise ratio (SNR) achievable when deriving synthetic photometry from the *Gaia* spectrophotometry, we perform some simulations according to the following guidelines:

The flux,  $F$ , in a given filter bandpass,  $T(\lambda)$ , is given by

$$F = \int_{\lambda_0}^{\lambda_1} T(\lambda) \cdot s(\lambda) d\lambda \quad , \quad (1)$$

where  $s(\lambda)$  is the source spectrum and  $\lambda_0 < \lambda < \lambda_1$  the applicable wavelength interval. This may be written as well as

$$F = \langle T | s \rangle \quad . \quad (2)$$

If  $\mathbf{s}$  is the vector of coefficients representing  $|s\rangle$  in a basis,  $B$ , of the solution space  $V^*$ , i.e.

$$s(\lambda) = \sum_{i=0}^{n-1} \mathbf{s}_i B_i(\lambda) \quad , \quad (3)$$

then we obtain

$$F = \sum_{i=0}^{n-1} \mathbf{s}_i \langle T | B_i \rangle \quad . \quad (4)$$

Introducing the vector  $\mathbf{t}$ , whose  $i$ -th element is  $\mathbf{t}_i = \langle T | B_i \rangle$ , the last expression becomes in short

$$F = \mathbf{t}^\top \mathbf{s} \quad . \quad (5)$$

Now let  $\Sigma^s$  be the covariance matrix of the vector  $\mathbf{s}$ . Then the variance on the flux in the filter bandpass is given by

$$\Sigma^F = \mathbf{t}^\top \Sigma^s \mathbf{t} \quad . \quad (6)$$

The covariance matrix  $\Sigma^s$  is obtained from the source calibration process.

After the application of the instrumental calibration derived using the set of pre-launch V0 SpectroPhotometric Standard Stars (SPSS, [7]), we build here the synthetic photometry for some preselected objects simulated with BaSeL-3.1 SED library [6]. Due to the limited range of wavelengths covered by this pre-launch SPSS release, in all computations here, the

<sup>2</sup><http://gaia.esac.esa.int/documentation/GDR1/index.html>.

<sup>3</sup>The planned dates for the *Gaia* release can be consulted in <http://www.cosmos.esa.int/web/gaia/release>.

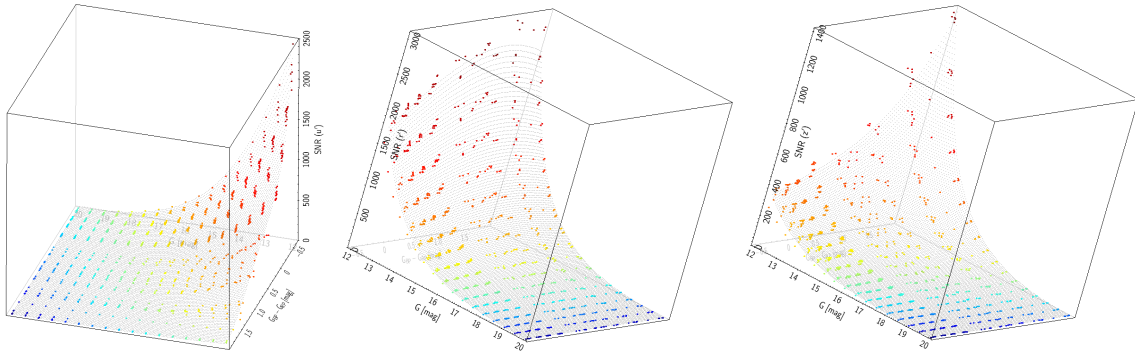


Figure 1: SNR surfaces fitted (grey) to the simulated BaSeL-3.1 data (coloured points) to derive a relationship with the colour and magnitude of the source for  $u'$  (left)  $r'$  (center) and  $z'$  Sloan passbands.

wavelength interval covers from  $\lambda_0 = 340$  nm to  $\lambda_1 = 920$  nm. So, a little of the UV sensitivity and some more IR *Gaia* sensitivity is missing in this analysis. Future SPSS releases will allow to extend this analysis to the full *Gaia* wavelength interval.

From BaSeL-3.1 dataset we selected a set of 54 sources covering  $4000 < T_{\text{eff}} < 45\,000$  K,  $1.5 < \log g < 5.0$ ,  $-2.0 < [\text{M}/\text{H}] < 0.5$ . To these sources, 17 DA type WDs were added covering  $5000 < T_{\text{eff}} < 40\,000$  K and  $7.0 < \log g < 9.0$ , extracted from [9].

Two noise components were added to the generated test observations, a normally distributed read-out noise component with  $\sigma = 6$   $e^-$  and Poisson-distributed photon noise. 70 observations (the average end-of-mission number of observations per *Gaia* source) in BP and RP, were generated and used for the calibration, at random location in the focal plane.

We used the nominal parameters for the Linear Spread Function (LSF<sup>4</sup>) and dispersion. The nominal overall response (optics/prisms/CCDs) was modified by an arbitrary function. The calibration is done using the first 15 principal components from the 94 SPSS of release V0 to construct the solution space.

Synthetic photometry in Sloan [3] and Johnson [1] systems, obtained from BaSeL-3.1 simulated dataset was used to derive fitted surfaces to get estimations of the SNR as a function of the magnitude and the colour of the source,  $\text{SNR} = f(G, G_{\text{BP}} - G_{\text{RP}})$  (see Sloan passband as examples in Fig. 1). These relationships are applied in Sect. 3 to different sky regions.

### 3 Number of calibrators in the sky

Every ground or space-based survey will be tracing a particular region in the sky. For instance, extragalactic surveys will concentrate its efforts at higher galactic latitudes to reduce the contamination by the stars in the Milky Way. Other surveys aiming to study the stellar content or exoplanets in the Galaxy will instead look carefully at the galactic disk, low

<sup>4</sup>The LSF is the 1D collapse of the PSF in the BP/RP spectra.

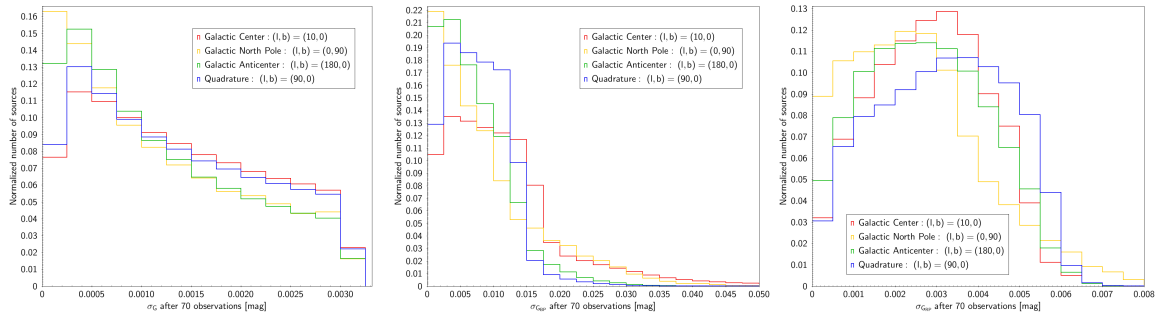


Figure 2: Normalised histogram of the end-of-mission photometric uncertainties expected at the different sky directions simulated for  $G$  (left),  $G_{BP}$  (center) and  $G_{RP}$  (right) passbands.

galactic latitudes. For this reason we study here four different directions in the sky using simulations of 4 degrees field of view each for stars with  $G < 20$ , obtained by the Besançon Galaxy Model adapted to the *Gaia* case [8]. These four regions in the sky are, a) the Galactic Center,  $l = 10^\circ$ ,  $b = 0^\circ$ , b) the quadrature,  $l = 90^\circ$ ,  $b = 0^\circ$ , c) the anticenter,  $l = 180^\circ$ ,  $b = 0^\circ$ , and d) the galactic north pole,  $l = 0^\circ$ ,  $b = 90^\circ$ . For every of these four sky regions, Table 1 shows their obtained stellar densities.

Table 1: Stellar densities,  $\rho$ , in stars-deg $^{-2}$ , obtained with [8] at different sky directions.

G	$\rho_{\text{center}}$	$\rho_{\text{quadrature}}$	$\rho_{\text{anticenter}}$	$\rho_{\text{pole}}$
<16	15766	17256	9052	454
16-17	15231	17167	6857	271
17-18	27295	28527	10921	407
18-19	48206	46642	15676	607
19-20	81088	76598	20832	868
All	187586	186204	63338	2607

Figure 2 shows the expected distribution of the associated uncertainties<sup>5</sup> to each *Gaia* passband ( $G$ ,  $G_{BP}$  and  $G_{RP}$ ) after 70 observations. As it can be seen all the sources in the different sky areas will have very good photometry at the end of the mission<sup>6</sup>, better than 3 mmag for  $G$ , 15 mmag for  $G_{BP}$  and 6 mmag for  $G_{RP}$ .

We can apply the SNR surfaces fitted in Sect. 2 to each of the sky regions under study to get an estimation of the number of stars with high SNR, potentially useful as standard sources for other observational programmes (Table 2). The corresponding percentage of sources is plotted in Fig. 3.

As it can be seen, the less favourable case ( $u'$  synthetic photometry in the quadrature direction) is able to provide about 314 stars-deg $^{-2}$ . On the other hand, the most favourable

<sup>5</sup> *Gaia* performances available in <http://www.cosmos.esa.int/web/gaia/science-performance> were used.

<sup>6</sup>  $G$  magnitudes have been already published for the 14 firsts months of data in the first *Gaia* data release.  $G_{BP}$  and  $G_{RP}$  are planned to be first published in the second release.

Table 2: Minimum and maximum percentage and density of sources with  $\text{SNR} > 50$  available in Sloan and Johnson synthetic filters studied in four different sky regions.

Filter	% interval	Stars $\cdot\text{deg}^{-2}$	Filter	% interval	Stars $\cdot\text{deg}^{-2}$
$u'$	4 – 17	314 – 6920	$U$	5 – 18	327 – 7249
$g'$	11 – 29	529 – 15 941	$B$	6 – 20	371 – 9324
$r'$	36 – 69	1023 – 54 728	$V$	23 – 47	809 – 34 207
$i'$	21 – 48	627 – 31 423	$R$	33 – 65	926 – 49 510
$z'$	16 – 44	533 – 24 293	$I$	20 – 49	608 – 30 248

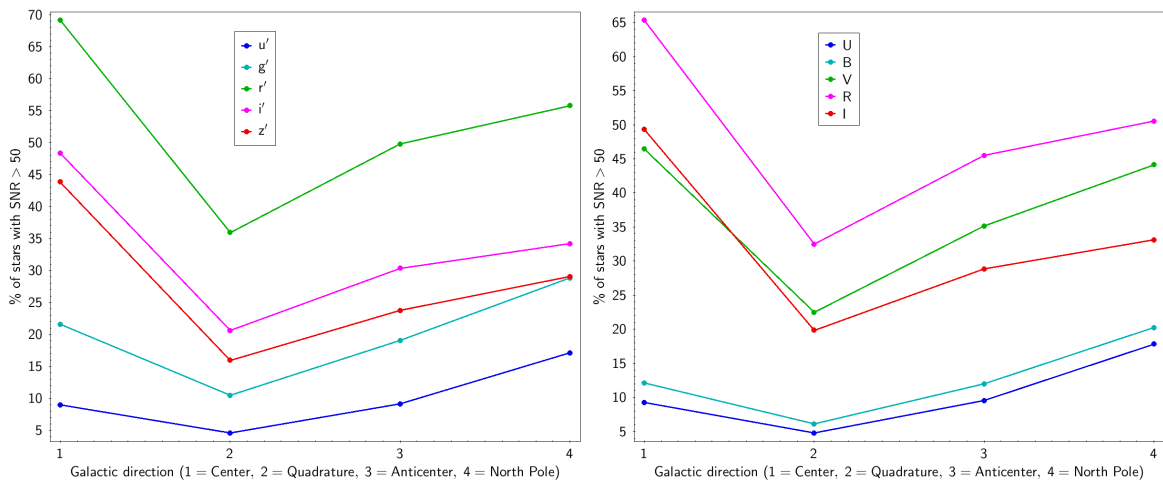


Figure 3: Percentage of sources with  $\text{SNR} > 50$  in every sky region analysed.

case is found when  $r'$  is synthesised from *Gaia* spectrophotometry in the galactic center direction, providing 54 728 stars $\cdot\text{deg}^{-2}$ . This means that, in whatever sky direction we look at, *Gaia* mission is able to provide enough sources with very high quality photometry that can be used as calibrators in other observing programmes.

## 4 Conclusions

We are used to hear that *Gaia* mission will revolutionise the astrometric studies with its microarcsecond positions and its derived parallaxes and proper motions. We have proved here how the *Gaia* photometric information will also provide very precise (at millimagnitude level) and homogeneous all-sky flux measurements for more than one billion sources that can potentially be used as standards in other observational programmes. The *Gaia* spectrophotometric information will be used to derive physical parameters and the continuous scanning during its 5 years of mission will also allow to perform variability studies for all these sources. The absolute flux calibration is aiming for the 1% accuracy level for all these sources, with an diffraction-limited angular resolution from space. For all these reasons, *Gaia* photometry

is unique and its photometric data will become the new reference in astronomy in the future.

## Acknowledgments

This work was supported by the MINECO (Spanish Ministry of Economy) - FEDER through grant ESP2014-55996-C2-1-R and MDM-2014-0369 of ICCUB (Unidad de Excelencia 'María de Maeztu').

## References

- [1] Bessell, M. S. 1990, *PASP*, 102, 1181
- [2] Carrasco et al 2016, in preparation
- [3] Fukugita, M., Ichikawa, T., Gunn, J. E., et al. 1996, *AJ*, 111, 1748
- [4] *Gaia* Collaboration, Prusti et al 2016, arXiv:1609.04153
- [5] Jordi, C., Gebran, M., Carrasco, J. M., et al. 2010, *A&A*, 523, A48
- [6] Lejeune, T., Cuisinier, F., & Buser, R. 1998, *A&AS*, 130, 65
- [7] Pancino, E., Altavilla, G., Marinoni, S., et al. 2012, *Monthly Notices of the Royal Astronomical Society*, 426, 1767
- [8] Robin, A. C., Luri, X., Reylé, C., et al. 2012, *A&A*, 543, A100
- [9] Tremblay, P.-E., Bergeron, P., & Gianninas, A. 2011, *ApJ*, 730, 128
- [10] van Leeuwen et al 2016, in preparation